Biochemical Pharmacology 80 (2010) 1528–1536

Contents lists available at ScienceDirect

Biochemical Pharmacology

journal homepage: www.elsevier.com/locate/biochempharm

# Induction of thymidine kinase 1 after 5-fluorouracil as a mechanism for 3′-deoxy-3′-[$^{18}$F]fluorothymidine flare

Seung Jin Lee [a], Seog Young Kim [a,b], Jin Hwa Chung [b], Seung Jun Oh [a,b], Jin Sook Ryu [a,b], Yong Sang Hong [c], Tae Won Kim [a,c], Dae Hyuk Moon [a,b,*]

[a] Institute for Innovative Cancer Research, Asan Medical Center, Asanbyeongwon-gil 86, Songpa-gu, Seoul 138-736, Republic of Korea
[b] Department of Nuclear Medicine, University of Ulsan College of Medicine, Asan Medical Center, Asanbyeongwon-gil 86, Songpa-gu, Seoul 138-736, Republic of Korea
[c] Department of Oncology, University of Ulsan College of Medicine, Asan Medical Center, Asanbyeongwon-gil 86, Songpa-gu, Seoul 138-736, Republic of Korea

ARTICLE INFO

*Article history:*
Received 15 May 2010
Accepted 9 August 2010

*Keywords:*
5-Fluorouracil
Thymidine kinase 1
Thymidylate synthase
Positron emission tomography
[$^{18}$F]fluorothymidine

ABSTRACT

Imaging the pharmacodynamics of anti-cancer drugs may allow early assessment of anti-cancer effects. Increases in 3′-deoxy-3′-[$^{18}$F]fluorothymidine ([$^{18}$F]FLT) uptake early after thymidylate synthase inhibition (TS) inhibition, the so-called flare response, is considered to be largely due to an increase in binding sites for type-1 equilibrative nucleoside transporter. We investigated the induction of thymidine kinase 1 (TK1) after 5-fluorouracil (5-FU) treatment as one of mechanisms for [$^{18}$F]FLT flare. Exposure of nine cancer cell lines to 5-FU for 24 h induced a 2.5- to 3.5-fold increase in [$^{18}$F]FLT uptake, significantly higher than the 1.5-fold increase observed 2 h after treatment. The increase of [$^{18}$F]FLT uptake 24 h after 5-FU exposure accompanied TK1 induction in most cell lines. In representative cell lines (A431 and HT29), 5-FU time-dependently increased [$^{18}$F]FLT uptake, kinase activity and the levels of protein and mRNA for TK1, sequential cyclin E and A induction, and $G_1$–S phase transition. Cycloheximide treatment and knockdown of TK1 completely inhibited 5-FU-induced [$^{18}$F]FLT flare. On the other hand, HCT8 cells showed a biphasic [$^{18}$F]FLT flare with lacked TK1 induction in response to the dosage of 5-FU. Cycloheximide did not inhibit 5-FU-induced [$^{18}$F]FLT flare in this cells. *In vivo* dynamic [$^{18}$F]FLT-PET and *ex vivo* analysis in HT29 tumor-bearing mice showed significantly increased [$^{18}$F]FLT flux and TK1 activity of tumor tissue 24 h after 5-FU administration ($P < 0.05$). Conclusively, 5-FU induced TK1 and TK1-mediated high [$^{18}$F]FLT flare in most of cell lines. [$^{18}$F]FLT-PET may be used to assess pharmacodynamics of TS inhibitor by a mechanism involving TK1 induction.



## 1. Introduction

Thymidylate synthase (TS), a folate-dependent enzyme that catalyzes a reaction required for the *de novo* synthesis of thymidylate, is a target for anti-cancer drugs [1–3]. Unfortunately, the expression levels of TS and folate receptors vary depending on cancer cell type, leading to often unsatisfactory therapeutic efficacy of agents targeting this enzyme. Even 5-FU, a representative TS inhibitor widely used for neo-adjuvant and metastatic chemotherapy in various solid tumors, has clinical response rates of only 10–15% when administered as monotherapy and 20–40% when administered in combination regimens [4–6].

The characterization of biological factors that correlate with response to TS inhibition may be important in identifying those patients who are most likely to benefit from treatment with TS inhibitors [1]. Alternatively, a method of predicting TS inhibition may be critical in the development of new TS inhibitors. Intratumoral levels of TS, thymidine phosphorylase, dihydropyrimidine dehydrogenase and other biomarkers have been associated with tumor response to 5-FU [1,7–9]. These methods, however, are invasive or may not give complete information about tumors.

TS inhibition was reported to increase the thymidine kinase 1 (TK1) activity and nucleoside transporter expression to regulate intracellular thymidine triphosphate pools [10], a mechanism attributed to an increase in salvage kinetics following TS inhibition. *In vitro* and *in vivo* positron emission tomography (PET) studies have demonstrated increases in radiolabeled thymidine or 3′-deoxy-3′-[$^{18}$F]fluorothymidine ([$^{18}$F]FLT) uptake early after TS inhibition, the so-called flare response [8,9,11–15]. Interestingly, in cancer cells, [$^{18}$F]FLT flare following TS inhibition was shown to be due largely to an increase in binding sites for type-1 equilibrative nucleoside transporter within hours after drug administration, but without changing TK1 protein levels [9,13]. In humans, increases in [$^{18}$F]FLT uptake after oral

* Corresponding author at: Department of Nuclear Medicine, University of Ulsan College of Medicine, Asan Medical Center, Asanbyeongwon-gil 86, Songpa-gu, Seoul 138-736, Republic of Korea. Tel.: +82 2 3010 4592; fax: +82 2 3010 4588.
*E-mail address:* dhmoon@amc.seoul.kr (D.H. Moon).

0006-2952/$ – see front matter © 2010 Elsevier Inc. All rights reserved.
doi:10.1016/j.bcp.2010.08.004

capecitabine treatment were also attributed to the redistribution of transporters [14]. To date, however, the role of TK1 has not been assessed, and the molecular mechanisms underlying [$^{18}$F]FLT flare in response to 5-FU have not been fully determined. We therefore investigated whether 5-FU treatment induces TK1, and whether TK1 mediates 5-FU-induced [$^{18}$F]FLT flare. We also assessed TK1-mediated [$^{18}$F]FLT flare using PET in mouse tumor model.

## 2. Materials and methods

### 2.1. Radiopharmaceutical preparation

[$^{18}$F]FLT was prepared from (5′-O-DMTr-2′-deoxy-3′-O-nosyl-b-D-threopentafuranosyl)-3-N-BOC-thymine by the nucleophilic fluorination of $^{18}$F-fluoride in a protic solvent (t-butanol or t-amyl alcohol) [16]. Typically, decay-corrected radiochemical yields ranged from 60% to 70%. The mean ± SD radiochemical purity was 98 ± 1.2%, with a specific activity greater than 60 TBq/mmol.

### 2.2. Cell culture, drug treatment, and preparation of cell lysates

A431, HT29, HeLa, MDA-MB-231, Calu6, A549, HCT116, MCF7, and HCT8 cell lines were obtained from the American Type Culture Collection. SNU-620 and SNU-620R-5-FU/1000 cell lines were purchased from Korea Cell Line Bank (Supplementary Table 1). Cells were maintained as manufacturer's recommendations and routinely seeded in 6-well plates to reach 80% confluency after 48 h. 5-FU (Sigma, St. Louis, MO), gemcitabine (Sigma, St. Louis, MO), or pemetrexed (Lilly, Indianapolis, IN) was exposed to cells 24 h after seeding. Cell lysates were prepared as described previously [17]. Protein content was determined by Bradford assay (Bio-Rad, Hercules, CA).

### 2.3. [$^{18}$F]FLT uptake assay

Twenty-four hours after seeding, exponentially growing cells were exposed to 5-FU for indicated time periods, followed by incubation for 2 h in 1 ml fresh medium containing 185 kBq of [$^{18}$F]FLT. The radioactivity in cells and supernatant was measured with a liquid scintillation counter (Perkin-Elmer, Waltham, MA). Viable cell number was counted with aliquot of cell fraction and used for the normalization of [$^{18}$F]FLT uptake. [$^{18}$F]FLT uptake was calculated as $100 \times CPM_{cell}/(CPM_{cell} + CPM_{sup})/1 \times 10^5$ cells. For Supplementary Fig. 2, we used [$^3$H]FLT (0.001 μCi/ml media) (Moravek Biochemicals, Brea, CA) for uptake test. In some experiments, 10 μg/ml cycloheximide (Sigma, St. Louis, MO) was incubated with 5-FU. To monitor the effects of TK1 knockdown, quadruplicate aliquots of growing cells in 96-well plate were transduced with lentivirus expressing shRNA for TK1 or non-target (MOI = 1) (Sigma, St. Louis, MO) in the presence of polybrene (Sigma, St. Louis, MO) 12 h before 5-FU treatment. All experiments were independently repeated 4–6 times.

### 2.4. TK1 activity measurement

TK1 activity was measured as previously described, with slight modifications [18]. Cells were lysed and sequentially centrifuged to isolate the cytosolic fraction. Each sample was mixed with an equal volume of reaction buffer containing [*methyl*-$^3$H]thymidine (Moravek Biochemicals, Brea, CA) and incubated at 37 °C with gentle stirring. The radioactivity of aliquots removed after 15, 30, and 60 min was measured and reported as picomoles of phosphorylated thymidine/minute/μg protein (pmol/min/μg) from time-activity curves.

### 2.5. Immunoblot analysis

SDS-polyacrylamide gel electrophoresis and immunoblot analysis were performed as described [17]. Antibody to TK1 was obtained from Abnova (Walnut, CA). Other antibodies were purchased from Santa Cruz Biotechnology (Santa Cruz, CA). Changes in expression level normalized by β-actin level were determined by scanning densitometry of immunoblots using Universal Hood II and Quantity One software (Bio-Rad, Hercules, CA).

### 2.6. Flow cytometric analysis

Cells treated with vehicle or 100 μM 5-FU for 18 h were trypsinized, fixed in 70% ethanol and stained with 4′,6-diamidino-2-phenylindole solution, and subjected to flow cytometry (Becton Dickinson, San Jose, CA). Data obtained from the Particle Analysis System were processed with ModFit LT software (Verity Software House, Topsham, ME).

### 2.7. Reverse transcription-real-time PCR

Total RNA was isolated using TRIzol reagent (Invitrogen, Carlsbad, CA) according to the manufacturer's instructions, and 2-μg of aliquots was reverse transcribed in mixtures containing AMV-reverse transcriptase, OligodT, dNTP, and RNAsin (Promega, Madison, WI). The resulting cDNAs were used for real-time PCR analysis using a SDS 7000 (Applied Biosystems, Foster City, CA) and specific primers for human TK1 and glyceraldehyde 3-phosphate dehydrogenase (Bioneer corporation, Daejon, Korea) [9]. Melting curve analysis was performed after amplification to verify the specificity of the amplicon.

### 2.8. Animals and tumor models

Athymic male nude mice (Balb-c/nu, aged 5.5 weeks) were purchased from Shizuoka Laboratory Center (Hamamatsu, Japan). All animal procedures were performed under the Institutional Animal Care and Use Committee guidelines of the Asan Institute for Life Science. Exponentially growing HT29 cells (0.2 ml containing $7 \times 10^6$ cells) were inoculated into the right flank of each mouse and grown to reach 80–120 mm$^3$ in volume. The mice with HT29 tumors underwent [$^{18}$F]FLT-PET before and 24 h after intraperitoneal administration of saline or maximum tolerated dose of 5-FU (165 mg/kg; $n = 8$ for each vehicle and 5-FU treatment group) (Choongwae Pharma, Seoul, Korea) [9]. Intraperitoneal injection was expected to result in the slow release of 5-FU from the peritoneal cavity, allowing mice to be exposed for prolonged periods of time [19]. TK1 activity was measured in another group of mice with HT29 tumors 24 h after saline or 5-FU treatment ($n = 6$ for each vehicle and 5-FU treatment group). TK1 activity was measured immediately after tumor isolation because we observed that TK1 activity was decreased to less than 20% of control levels by snap-freezing or overnight storage at 4 °C (unpublished data).

### 2.9. Animal PET imaging and analysis

A commercially available PET system (Focus 120 microPET, Siemens Inc., Knoxville, TN) was used [20,21]. One-hour dynamic PET scans were obtained after tail vein injection of 7.4 MBq (0.2 mCi) [$^{18}$F]FLT and the data were analyzed using PMOD software (version 2.65; PMOD Group, Zurich, Switzerland) according to a three-compartment model with four parameters [20]. Parameters $K_1$ and $k_2$ are rate constants for forward and reverse transport of [$^{18}$F]FLT between plasma and tissue pool, respectively. The rate constant $k_3$ represents thymidine kinase-mediated phosphorylation of [$^{18}$F]FLT. The standardized uptake

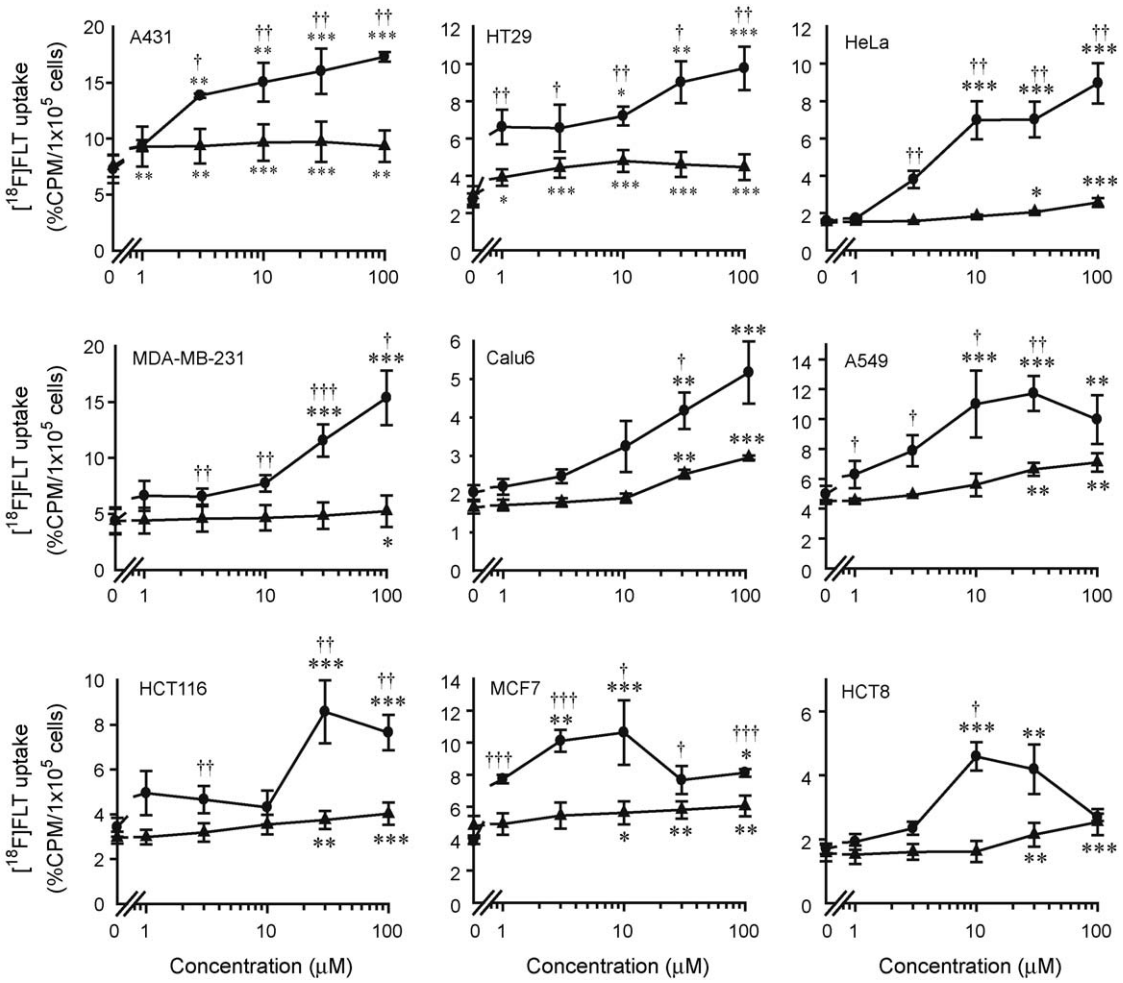


**Fig. 1.** Effect of 5-FU on changes in [$^{18}$F]FLT uptake in nine cancer cell lines. Cells were treated with vehicle or 5-FU at indicated concentrations for 2 h (triangle dots) or 24 h (circle dots), and exposed to [$^{18}$F]FLT for another 2 h. [$^{18}$F]FLT uptake was normalized with the viable cell number after 5-FU treatment and expressed as %CPM/1 $\times$ $10^5$ cells. All data represent the mean $\pm$ SE of 4–6 independent experiments. $^{*}P < 0.05$; $^{**}P < 0.01$; $^{***}P < 0.001$; compared with vehicle-treated samples. $^{\dagger}P < 0.05$; $^{\dagger\dagger}P < 0.01$; $^{\dagger\dagger\dagger}P < 0.001$; compared with samples treated with the same concentration of 5-FU for 2 h.

value (*SUV*) of each tumor was calculated from the last frame of the dynamic study (50 min after injection) using the formula: $SUV_{mean}$ = (tumor radioactivity in the tumor volume of interest with the unit of Bq/cc $\times$ body weight) divided by injected radioactivity. The net influx constant ($K_{FLT}$) was calculated as:

$$K_{FLT} = \frac{K_1 k_3}{K_1/V_d + k_3}$$

### 2.10. Statistical analysis

Repeated measures analysis of variance was used to assess significant differences between groups. Treatments were compared using the Student's *t*-test. [$^{18}$F]FLT-PET parameters were analyzed using the Wilcoxon signed-rank test and the Mann–Whitney *U*-test. $P < 0.05$ was considered statistically significant.

## 3. Results

### 3.1. 5-FU induced changes in [$^{18}$F]FLT uptake in cancer cell lines

A431, HT29, HeLa, MDA-MB-231, Calu6, A549, HCT116, MCF7, and HCT8 cells were grown for 24 h, and exposed to vehicle or 1, 3, 10, 30, or 100 μM 5-FU for 2 or 24 h; [$^{18}$F]FLT uptake and cell count were then measured. The tested cells were sensitive to 5-FU, having $IC_{50}$ within the ranges of tested concentrations (Supplementary Fig. 1). The viable cell number was minimally changed after 2 h treatment, and dose-dependently decreased by 24 h (Supplementary Table 2). In most cell lines, [$^{18}$F]FLT uptake was significantly dependent on the concentration of 5-FU ($P < 0.05$, Fig. 1A) 24 h after treatment. Exposure of A431, HT29, HeLa, MDA-MB-231, and Calu6 cells to 100 μM 5-FU increased average [$^{18}$F]FLT uptake 3.54 $\pm$ 0.60-fold, whereas exposure to 10 μM 5-FU increased uptake 2.46-fold. In A549, HCT116, MCF7 and HCT8 cells, [$^{18}$F]FLT uptake reached a plateau at 10–30 μM 5-FU with a 2.58 $\pm$ 0.08-fold increase. With 100 μM 5-FU, however, a significant decrease in [$^{18}$F]FLT uptake was observed in MCF-7 and HCT8 cells ($P < 0.05$).

Two-hour exposure to 5-FU also significantly increased [$^{18}$F]FLT uptake ($P < 0.05$), but the magnitude of change was differed significantly from that observed after 24 h in most cell types (Fig. 1A). Two-hour exposure to 1 μM 5-FU increased [$^{18}$F]FLT uptake compared to vehicle in A431 and HT29 cells, whereas treatment with 100 μM 5-FU for 2 h was required to induce uptake in MDA-MB-231 cells. The average maximum increase in all cell lines was 1.48-fold.

### 3.2. 5-FU induction of TK1 expression

All cells showed greater [$^{18}$F]FLT uptake after 24 h than after 2 h of 5-FU exposure; hence, we assessed the molecular changes

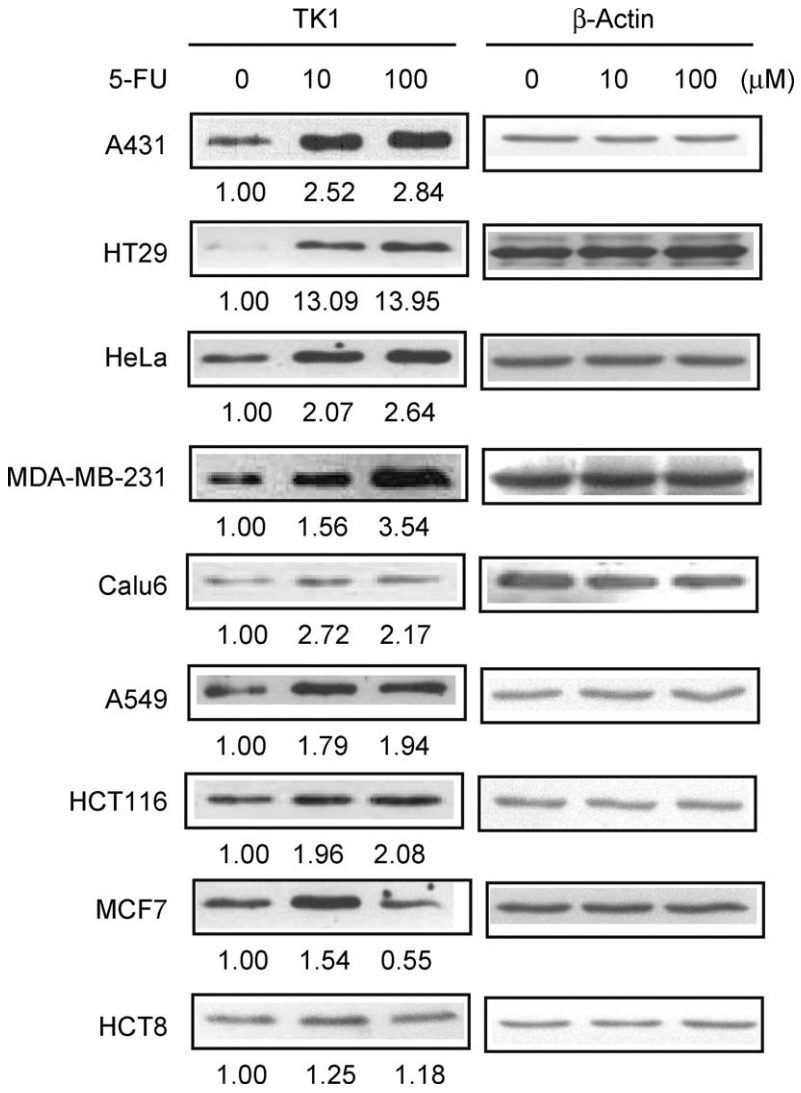


**Fig. 2.** TK1 expression after 5-FU treatment. Exponentially growing cells were treated with vehicle or 5-FU at the indicated concentrations for 18 h.

associated with [$^{18}$F]FLT flare in cells exposed to 5-FU for 24 h. Cells were treated with 10 or 100 μM 5-FU for 24 h and subjected to Western-blot analysis to detect TK1 and β-actin. TK1 expression was dose-dependently increased by 5-FU treatment in A431, HT29, HeLa, and MDA-MB-231 cells (Fig. 2). Calu6, A549 and HCT116 cells showed the comparable degree of TK1 induction after exposure to both concentrations of 5-FU. In MCF7 cells, TK1 was induced at 10 μM, but decreased at 100 μM. TK1 expression was not significantly changed by 5-FU in HCT8 cells. All cell lines showed an increased expression in TS or ternary complex of TS with FdUMP and 5,10-methylene-tetrahydrofolate in response to 5-FU, but any common patterns were observed. These data indicated that 5-FU can up-regulate TK1 expression in most of tested cells, but not in HCT8 cells.

### 3.3. 5-FU-induced [$^{18}$F]FLT uptake and TK1 expression in 5-FU-resistant cell line

Effect of 5-FU on [$^{18}$F]FLT uptake and TK1 expression was compared in 5-FU sensitive and resistant cell lines to investigate whether 5-FU-induced changes are observed only in a 5-FU-sensitive cell line (Supplmentary Fig. 2). SNU-620 cells showed an $IC_{50}$ that is within the range of tested 5-FU concentrations while relative cell death of SUN-620R-5-FU/1000 exposed to 30 μM of 5-FU was less than 0.14. 5-FU increased [$^{3}$H]FLT uptake of 1.96-fold and TK1 expression in 5-FU-sensitive SUU-620 cells. On the contrary, change in [$^{3}$H]FLT uptake and induction of TK1 were not observed in SUN-620R-5-FU/1000 cells

### 3.4. Time-dependent changes of [$^{18}$F]FLT uptake and TK1 activity by 5-FU

In order to investigate the role of TK1 induction for [$^{18}$F]FLT uptake, we performed subsequent experiments in three representative cell lines: A431, HT29 and HCT8. We measured time-dependent changes in [$^{18}$F]FLT uptake and TK1 activity with 100 μM 5-FU. Both A431 and HT29 cells showed time-dependent increases in [$^{18}$F]FLT and TK1 activity (Fig. 3A and B). In A431 cells, [$^{18}$F]FLT uptake tended to increase gradually at 2 h and significantly at 18 and 24 h ($P < 0.001$). TK1 activity was also significantly increased at 24 h ($P < 0.05$). In HT29 cells, [$^{18}$F]FLT uptake was significantly increased, in parallel with TK1 activity, beginning at 2 h of 5-FU treatment ($P < 0.001$). HCT8 cells showed an increase in [$^{18}$F]FLT uptake ($P < 0.001$), but this change was not paralleled by TK1 activity change. We confirmed that treatment with vehicle did not induce significant changes in [$^{18}$F]FLT uptake and TK1 activity over this period (data not shown).

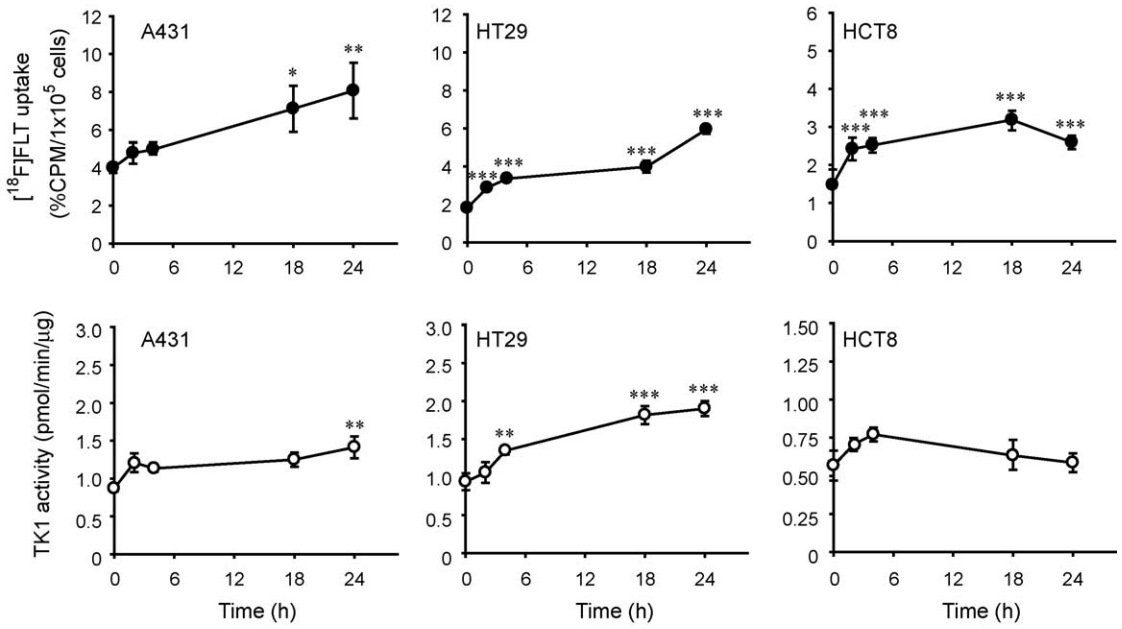


**Fig. 3.** Effect of 5-FU on [$^{18}$F]FLT uptake and TK1 activation in A431, HT29 and HCT8 cells. 100 μM 5-FU-induced time-dependent changes in [$^{18}$F]FLT uptake (A) and TK1 activity (B). Data expressed as mean ± SE of four separate experiments. $^{*}P < 0.05$; $^{**}P < 0.01$; $^{***}P < 0.001$; compared with the samples of 0 h.

### 3.5. Selective induction of TK1 during $G_1S$ transition by 5-FU

We assessed 5-FU-induced changes in cell-cycle distribution and TK1 expression in A431, HT29 and HCT8 cells. TK1 expression in A431 and HT29 cells was increased in a time-dependent manner by treatment with 5-FU (Fig. 4A). In A431 cells, cyclin E, and subsequently cyclin A, were induced, beginning 18 h after exposure to 5-FU, along with an increase in TK1. As cyclin E is still up-regulated until 24 h and the proportions in cells in $G_0G_1$ and S phases were increased by 14% and 21%, respectively, 5-FU was supposed to increase the fraction of cells in late $G_1$-early S phase (Fig. 4B). Increase in TK1 protein levels accompanied the increase in TK1 mRNA levels (Fig. 4C), which indicated that TK1 was transcriptionally up-regulated during $G_1S$ transition in A431 cells. Similar to the results in A431 cells, HT29 cells showed increases in cyclin A and TK1 mRNA levels. The decreases in cyclin E levels and accumulation in S phase, indicating that 5-FU also induced S-phase arrest. After 5-FU treatment for 18 h, HCT8 cells also showed a significant increase in cyclin A level and accumulation in S phase. However, the TK1 protein level was not significant change in any time point and the mRNA level was decreased (Fig. 4A and C) in these cells. We next examined whether other anti-metabolite drug those are known to inhibit TS [22,23] could induce TK1 expression in HT29 cells (Fig. 4D) as deoxycytidine analogues (gemcitabine) and anti-folates (BGC 945, pemetrexed) are also implicated in [$^{18}$F]FLT flare [11,13]. Exposure of 300 nM gemcitabine and pemetrexed to HT29 cells increased the expression levels of TK1 and cyclin A from 6 h and the increases persisted up to 24 h. These data suggested that TK1 and cyclin A expression is generally regulated by anti-metabolite agents in this cell type.

### 3.6. Requirement of TK1 for 5-FU-induced [$^{18}$F]FLT flare

Treatment with cycloheximide plus 100 μM 5-FU for 18 h completely inhibited 5-FU-induced [$^{18}$F]FLT flare in A431 and HT29 cells ($P < 0.01$, Fig. 5A) but not in HCT8 cells. Cycloheximide also inhibited 5-FU-induced TK1 expression in A431 and HT29 cells (Fig. 5A). To verify the role of TK1 in these cells, we infected cells with lentivirus encoding TK1-specific shRNA. This resulted in the specific down-regulation of TK1 mRNA levels, to less than 10% of control levels, as demonstrated by real-time PCR analysis (Fig. 5B, right). 5-FU changed [$^{18}$F]FLT uptake by 0.50- and 1.46-fold, respectively, in A431 and HT29 cells transduced with this virus (MOI = 1), compared with 2.33- and 2.64-fold in A431 and HT29 cells transduced with lentivirus encoding scrambled shRNA, respectively (Fig. 5B).

### 3.7. Imaging of TK1-mediated [$^{18}$F]FLT uptake in 5-FU-treated mice

The [$^{18}$F]FLT uptake in HT29 tumors was markedly enhanced by 24-h treatment with 5-FU but not by saline (Fig. 6A). The $SUV_{mean}$ was unchanged over time in the saline-treated group (0.93 ± 0.12 vs. 0.87 ± 0.12), but increased markedly (2.57-fold increase) in the 5-FU-treated group (0.88 ± 0.13 vs. 2.26 ± 0.42, $P < 0.05$) (Fig. 6B and Supplementary Table 3). Quantitative assessment of the time-activity curve of [$^{18}$F]FLT uptake revealed that $K_{FLT}$, $k_3$ and $K_1/k_2$ were significantly increased after 24 h treatment with 5-FU ($P < 0.05$) (Fig. 6B and Supplementary Table 3). We monitored the change of TK1 activity by 5-FU in HT29 tumor. The relative TK1 activity of 5-FU-treated HT29 tumors was 1.49 ± 0.11, which was significantly higher than that of vehicle-treated tumors (1.00 ± 0.15) ($P < 0.05$, Fig. 6C).

## 4. Discussion

To our knowledge, this study is the first to show that TK1 mediates the increase in [$^{18}$F]FLT uptake induced by 5-FU treatment, both *in vivo* and *in vitro*. The high [$^{18}$F]FLT flare occurring 24 h after 5-FU treatment was accompanied by an increase in TK1 expression in most cell lines. 5-FU-resistant cells, SNU-620-5-FU/1000, showed no changes in [$^{3}$H]FLT uptake and TK1 expression. TK1 was activated during the $G_1S$ cell-cycle transition and TK1 activation was crucial for the [$^{18}$F]FLT flare, as demonstrated by treatment with cycloheximide and TK1 knock-down. The increased [$^{18}$F]FLT influx ($K_{FLT}$) in mice after 5-FU treatment was accompanied by an increase in TK1 activity in tumor samples, indicating that 5-FU activation of TK1 can be assessed by measuring [$^{18}$F]FLT flare *in vivo*.

Understanding the molecular mechanisms underlying selective TK1 activation by 5-FU is important in determining whether TK1 activation can be used as an imaging biomarker to assess TS

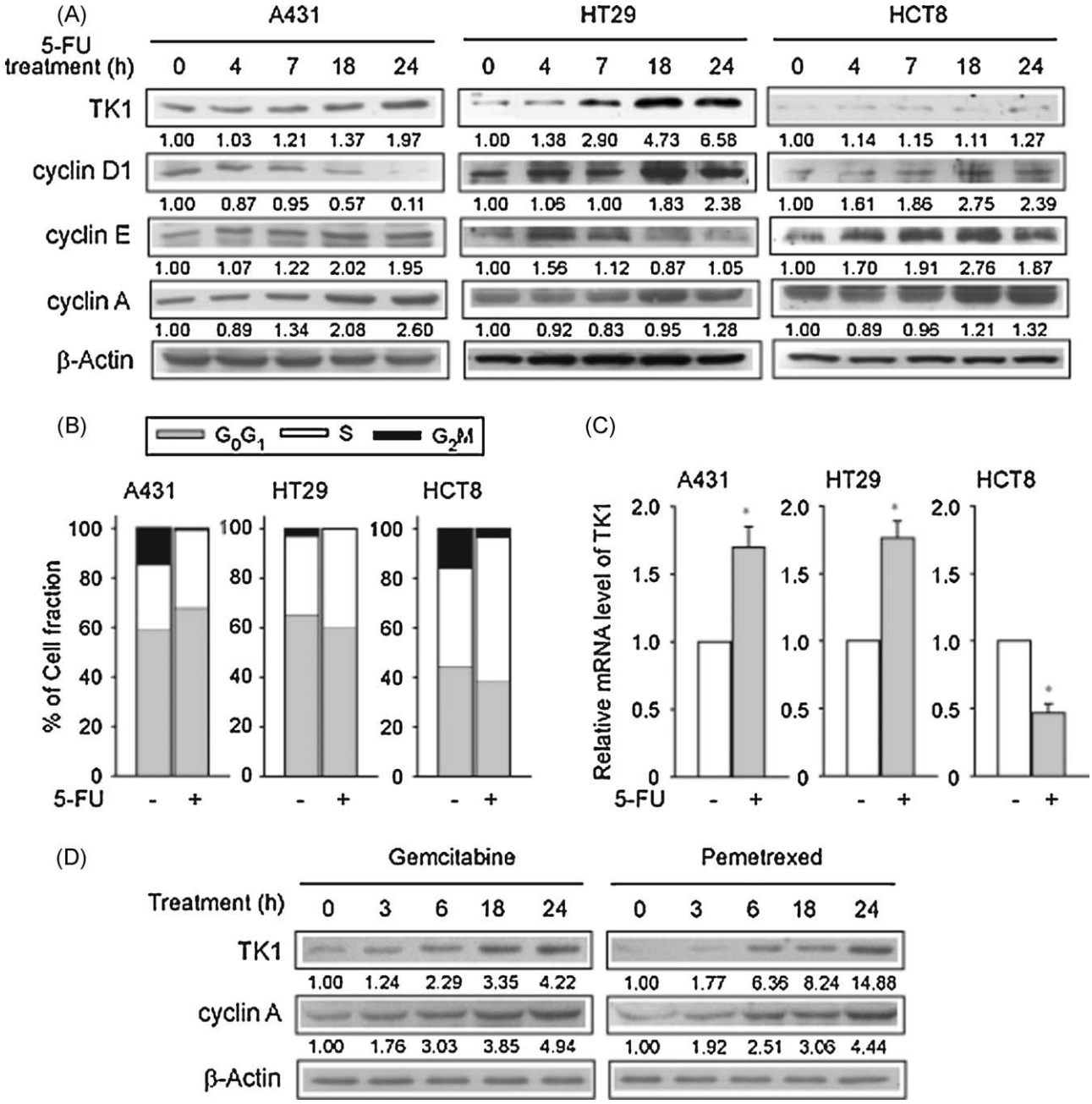


**Fig. 4.** Effect of 5-FU on cell-cycle transition in A431, HT29 and HCT8 cells. (A) Time-dependent changes in the expression of TK1, cyclin D1, cyclin E, cyclin A, and β-actin by 100 μM 5-FU. The changes in cell-cycle distribution (B) and TK1 mRNA levels (C) by 100 μM 5-FU. Cells treated for 18 h with vehicle or 5-FU were subjected to FACS and reverse transcription-real-time PCR analysis. Data were confirmed with three independent experiments and expressed as mean ± SE. $^{*}P < 0.05$; compared with vehicle-treated samples. (D) Time-dependent changes in the expression of TK1, cyclin A, and β-actin by 300 nM gemcitabine (left) and pemetrexed (right) in HT29 cells.

inhibition. Our data suggest that TK1 induction is a pharmacodynamic event directly resulting from the 5-FU-induced signal cascade. Importantly, we also observed [$^{18}$F]FLT flare with TK1 induction after gemcitabine and pemetrexed that are known to inhibit TS *in vivo*. We found that 5-FU increased cyclin A and TK1 mRNA levels and the number of cells in $G_1$ and/or S phase. 5-FU activates Chk1 which mediates Cdc25A proteolysis, leading to Cdk2 inhibition [24]. As Cdk2 complexes with cyclin E or cyclin A, 5-FU can act at the $G_1$S transition or early S-phase arrest. Our results suggest that sequentially activated E2F1 or cyclin A during $G_1$S transition [25,26] would contribute to the transcriptional activation of TK1. Previously, TK1 activation by 5-FU was thought to be a regulatory mechanism sensitive to the depletion of endogenous thymidine triphosphate resulting from TS inhibition [10], and may ultimately result in resistance to anti-metabolite drugs [1,27]. Whether or not a thymidine salvage pathway contributes to clinical resistance to 5-FU has not yet been determined [27,28], but it likely that, at clinically relevant doses, a salvage pathway may not affect resistance to 5-FU [15,29]. Although our results indicate that [$^{18}$F]FLT flare can be mediated by a mechanism involving increased TK-1, it remains to be determined whether [$^{18}$F]FLT flare by TK1 is a pharmacodynamic biomarker of 5-FU inhibition of TS *in vivo*.

We also found that cell lines did not always up-regulate TK1 expression in response to 5-FU. MCF7 cells showed a biphasic [$^{18}$F]FLT flare. This biphasic increase in [$^{18}$F]FLT uptake in MCF7 may be due to a mixed mechanism [11] as like gemcitabine-induced biphasic changes in [$^{18}$F]FLT uptake which may be due to the

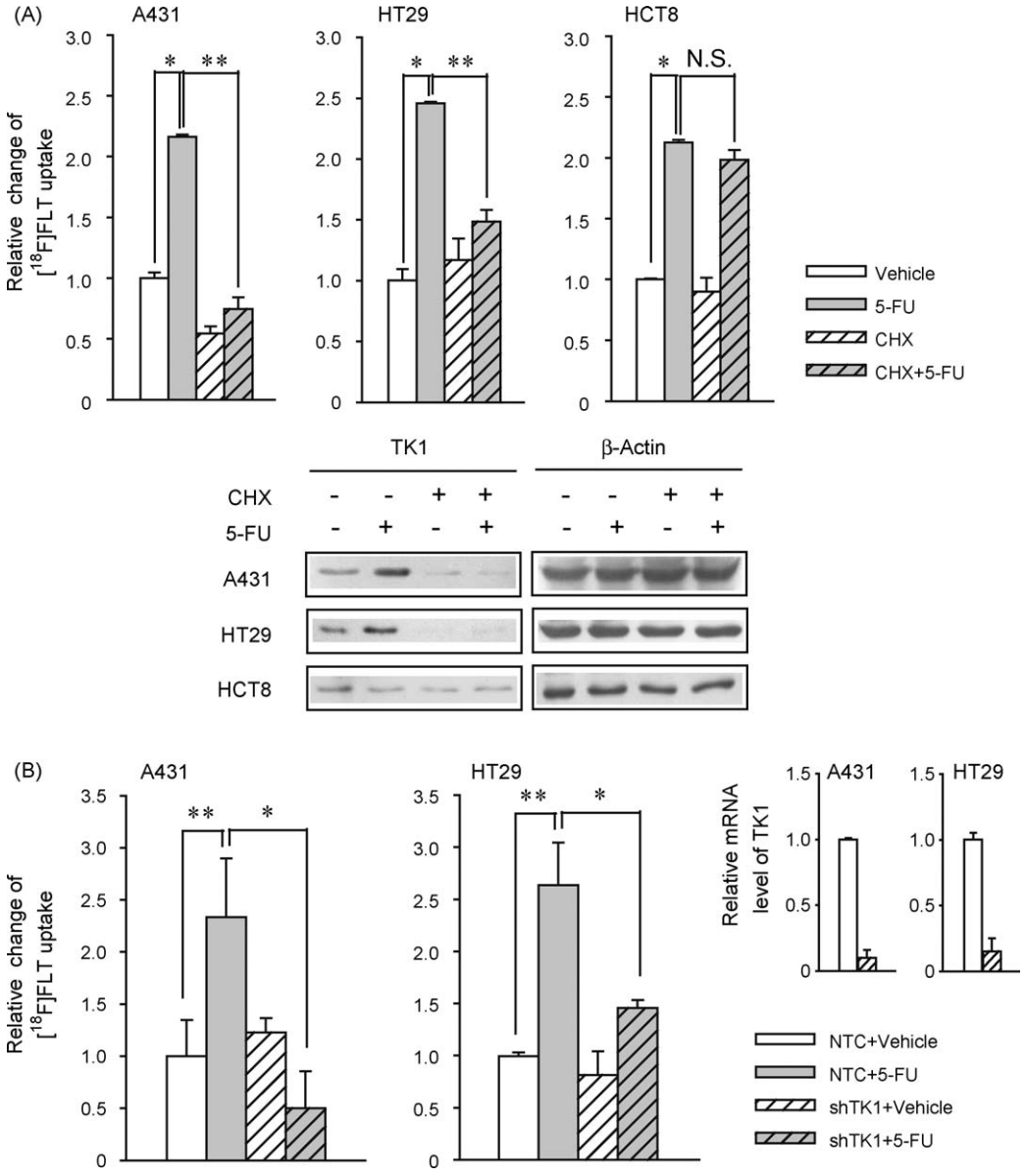


**Fig. 5.** The role of TK1 in 5-FU-induced [$^{18}$F]FLT uptake. (A) Effects of cycloheximide on 5-FU-induced [$^{18}$F]FLT uptake in A431, HT29, and HCT8 cells. Cells were treated with vehicle or 100 μM 5-FU in the absence or presence of 10 μg/ml cycloheximide for 18 h and subjected to [$^{18}$F]FLT uptake (upper) or Western-blot analyses (lower) ($n$ = 4). (B) Effect of TK1 knockdown (right) on 5-FU-induced [$^{18}$F]FLT uptake (left) in A431 and HT29 cells ($n$ = 4). Data represent mean ± SE. *$P < 0.05$. **$P < 0.01$. N.S.: not significant, NTC: non-targeted control.

activation of a salvage pathway at a moderate drug dose and direct DNA termination at higher concentrations [11]. HCT8 cells also showed a biphasic [$^{18}$F]FLT flare without TK1 induction. Treatment with cycloheximide plus 5-FU did not inhibit 5-FU-induced [$^{18}$F]FLT flare. As the observed [$^{18}$F]FLT flare was not correlated with TK1 expression change in HCT8 cells, it may be explained by a mechanism involving the redistribution of nucleoside transporters [9]. The reason for the failure in TK1 induction by 5-FU in HCT8 cell is thought that the transcriptional activation of TK1 at 5-FU-induced mitotic arrest may not be sufficient in HCT8 cells. Another possibility is RNA-mediated cellular toxicity. 5-FU is metabolized by orotate phosphoribosyl transferase to form 5-fluorouridine-5 monophosphate, which is phosphorylated to 5-fluorouridine triphosphate and inhibits RNA biosynthesis. As HCT8 cell has a higher ratio of uridine kinase to TK1 than many other cell lines [30], HCT8 cells may have been damaged by a RNA-mediated pathway. If RNA mediates cellular toxicity without TK1 induction, cells would susceptible to 5-FU with limited activation of TK1.

[$^{18}$F]FLT flares observed soon after TS inhibition [8,9,12–14] may be largely due to redistribution of the type-1 equilibrative nucleoside transporter [9,13]. The ability to assess pharmacodynamic changes as early as 1–2 h after TS administration is an important advantage, however, [$^{18}$F]FLT flares caused by a mechanism involving the redistribution of transporter may have some disadvantages. Assessments may be affected by the pharmacokinetics of the drug and may require the establishment of an optimal imaging window for PET to capture the peak level [14]. In addition, TS inhibitors may not be administered immediately after a baseline scan, because [$^{18}$F]FLT-PET performed after 1–2 h is affected by baseline [$^{18}$F]FLT activity [20]. In fact, in previous studies post-treatment and baseline [$^{18}$F]FLT-PET scans were not compared in the same mice [9,13]. More importantly, as shown here, TS inhibition may provoke a smaller [$^{18}$F]FLT flare after 1–2 h than after 24 h of exposure to 5-FU. Together with the observation that the plasma concentration during continuous infusion of 5-FU is 5–10 μM [31,32], *in vivo* [$^{18}$F]FLT-PET scans may

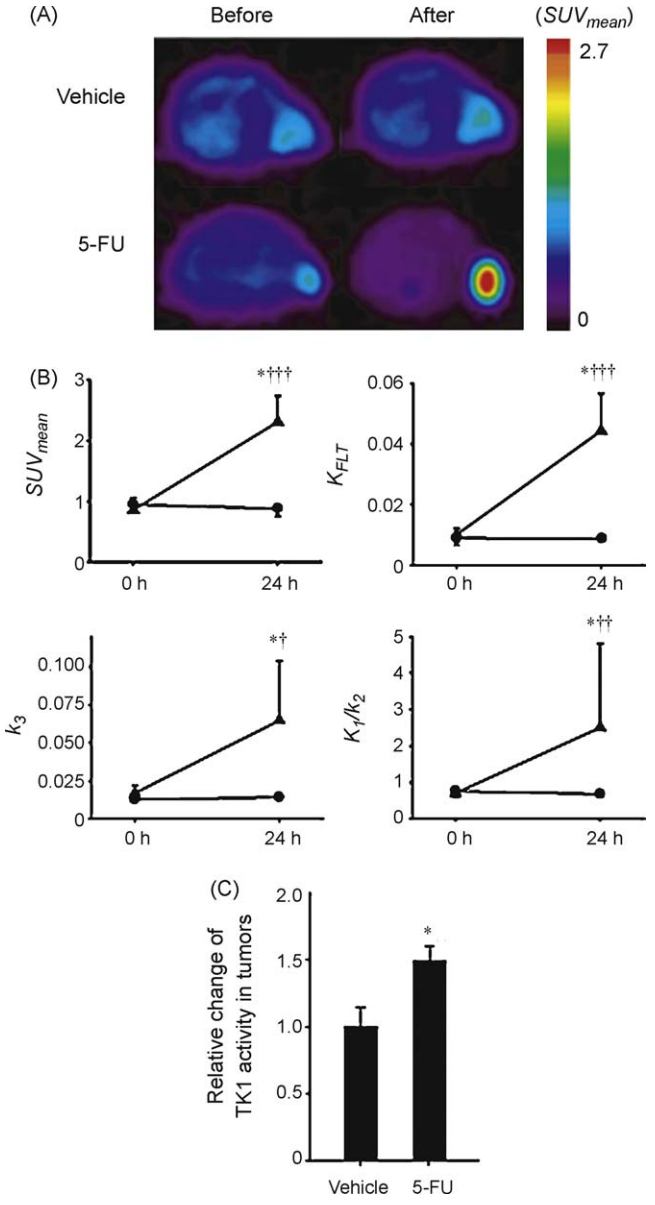


**Fig. 6.** Imaging of TK1-mediated [$^{18}$F]FLT uptake by 5-FU in mice with HT29 tumors. (A) Typical transverse [$^{18}$F]FLT-PET scan. (B) Changes in $SUV_{mean}$ and kinetic parameters ($K_{FLT}$, $k_3$, and $K_1/k_2$) in saline- (circle) or 5-FU- (triangle) treated mice bearing HT29 tumors ($n = 8$/group). Data expressed as mean ± SD. $^{*}P < 0.05$, compared with the value at 0 h. $^{\dagger}P < 0.05$, $^{\dagger\dagger}P < 0.01$, and $^{\dagger\dagger\dagger}P < 0.001$, comparison between the change over 24 h in vehicle-treated mice and that in 5-FU-treated mice. (C) Relative change of TK1 activity 24 h after vehicle or 5-FU treatment ($n = 6$/group). Data expressed as mean ± SE. $^{*}P < 0.05$ compared with vehicle-treated tumors.

be optimal after 24 h of treatment when continuous infusion of 5-FU is given. Our [$^{18}$F]FLT-PET results showed increases in kinetic as well as in static parameters that reflect [$^{18}$F]FLT retention. Our results indicate that delayed static [$^{18}$F]FLT-PET imaging can be used in future clinical or animal imaging studies to assess TK-1-induced [$^{18}$F]FLT flare [14].

We measured [$^{18}$F]FLT flare 24 h after administration of 5-FU. However, an increase in [$^{18}$F]FLT uptake reflecting TS inhibition may obscure the anti-proliferation effect of 5-FU [9,33]. In contrast to our results, previous studies have found that [$^{18}$F]FLT uptake by RIF-1 and HT29 cells was significantly lower 24 h after treatment with 5-FU vs. vehicle [8,33]. One reason may be that [$^{18}$F]FLT uptake was not adjusted for viable cell counts [8]. More importantly, cell viability or tumor proliferation assessed immunohistochemically significantly decreased 24 h after treatment with high 5-FU concentration. [$^{18}$F]FLT flare should be assessed at early time points, when cell viability is not compromised [9], with an optimal window that may depend on drug dose and pharmacokinetics [8,9,13,14]. Our results suggest that 24 h imaging may be optimal to assess TK-1-induced [$^{18}$F]FLT flare when low doses of 5-FU are infused continuously over several days. Imaging on later time points would limit the detection of [$^{18}$F]FLT flare because of increasing number of nonviable tumor cells in tumor tissue.

This study had several limitations. We did not evaluated the role of nucleoside transporter in [$^{18}$F]FLT flare because this was beyond the scope of our study. Redistribution of nucleoside transporters to the cell membrane may have contributed to [$^{18}$F]FLT flare. However, [$^{18}$F]FLT flare observed 24 h after 5-FU administration in this animal model may be largely due to TK1 induction as transporter mediated flare is usually observed soon after 5-FU administration. Second, [$^{18}$F]FLT-PET imaging of TKI induction may be applicable only to tumors in which this enzyme can be induced, or only after 5-FU continuous infusion, thus limiting the applicability of [$^{18}$F]FLT flare mediated by TK1. Finally, we have observed TS expression in all cell lines, but did not find the same TS expression patterns. The differential TS expression by 5-FU in various cell types had previously been reported through several literatures [34,35].

In conclusion, our results indicate that 5-FU treatment leads to TK1 induction and TK1 mediates 5-FU-induced [$^{18}$F]FLT flare in most cancer cell lines. Further studies should provide insights on [$^{18}$F]FLT flare mediated by TK1 induction as an imaging endpoint in assessing the anti-tumor effects of TS inhibitors.

## Acknowledgments

This study was supported by a grant of the Korea Healthcare Technology R&D Project, Ministry for Health, Welfare & Family Affairs, Republic of Korea (No. A062254) and by the Real Time Molecular Imaging Research Program (No. 2010-002040) of National Research Foundation, which is funded by the Ministry of Education, Science and Technology, Republic of Korea.

We thank Woo Yeon Moon, Haeng Jung Lee, Hye Young Kang, Sang Ju Lee, and Na Young Chung for excellent technical assistance.

## Appendix A. Supplementary data

Supplementary data associated with this article can be found, in the online version, at doi:10.1016/j.bcp.2010.08.004.

## References

[1] Longley DB, Harkin DP, Johnston PG. 5-Fluorouracil: mechanisms of action and clinical strategies. Nat Rev Cancer 2003;3:330–8.
[2] Walko CM, Lindley C. Capecitabine: a review. Clin Ther 2005;27:23–44.
[3] Jackman AL, Theti DS, Gibbs DD. Antifolates targeted specifically to the folate receptor. Adv Drug Deliv Rev 2004;56:1111–25.
[4] Macdonald JS, Gohmann JJ. Chemotherapy of advanced gastric cancer: present status, future prospects. Semin Oncol 1988;15:42–9.
[5] Rougier P, Van Cutsem E, Bajetta E, Niederle N, Possinger K, Labianca R, et al. Randomised trial of irinotecan versus fluorouracil by continuous infusion after fluorouracil failure in patients with metastatic colorectal cancer. Lancet 1998;352:1407–12.
[6] Douillard JY, Cunningham D, Roth AD, Navarro M, James RD, Karasek P, et al. Irinotecan combined with fluorouracil compared with fluorouracil alone as first-line treatment for metastatic colorectal cancer: a multicentre randomised trial. Lancet 2000;355:1041–7.
[7] Salonga D, Danenberg KD, Johnson M, Metzger R, Groshen S, Tsao-Wei DD, et al. Colorectal tumors responding to 5-fluorouracil have low gene expression levels of dihydropyrimidine dehydrogenase, thymidylate synthase, and thymidine phosphorylase. Clin Cancer Res 2000;6:1322–7.
[8] Yau K, Price P, Pillai RG, Aboagye E. Elevation of radiolabelled thymidine uptake in RIF-1 fibrosarcoma and HT29 colon adenocarcinoma cells after treatment with thymidylate synthase inhibitors. Eur J Nucl Med Mol Imaging 2006;33:981–7.
[9] Perumal M, Pillai RG, Barthel H, Leyton J, Latigo JR, Forster M, et al. Redistribution of nucleoside transporters to the cell membrane provides a novel

approach for imaging thymidylate synthase inhibition by positron emission tomography. Cancer Res 2006;66:8558–64.
[10] Pressacco J, Mitrovski B, Erlichman C, Hedley DW. Effects of thymidylate synthase inhibition on thymidine kinase activity and nucleoside transporter expression. Cancer Res 1995;55:1505–8.
[11] Dittmann H, Dohmen BM, Kehlbach R, Bartusek G, Pritzkow M, Sarbia M, et al. Early changes in [$^{18}$F]FLT uptake after chemotherapy: an experimental study. Eur J Nucl Med Mol Imaging 2002;29:1462–9.
[12] Wells P, Aboagye E, Gunn RN, Osman S, Boddy AV, Taylor GA, et al. 2-[$^{11}$C]thymidine positron emission tomography as an indicator of thymidylate synthase inhibition in patients treated with AG337. J Natl Cancer Inst 2003;95:675–82.
[13] Pillai RG, Forster M, Perumal M, Mitchell F, Leyton J, Aibgirhio FI, et al. Imaging pharmacodynamics of the alpha-folate receptor-targeted thymidylate synthase inhibitor BGC 945. Cancer Res 2008;68:3827–34.
[14] Kenny LM, Contractor KB, Stebbing J, Al-Nahhas A, Palmieri C, Shousha S, et al. Altered tissue 3′-deoxy-3′-[$^{18}$F]fluorothymidine pharmacokinetics in human breast cancer following capecitabine treatment detected by positron emission tomography. Clin Cancer Res 2009;15:6649–57.
[15] Direcks WG, Berndsen SC, Proost N, Peters GJ, Balzarini J, Spreeuwenberg MD, et al. [$^{18}$F]FDG and [$^{18}$F]FLT uptake in human breast cancer cells in relation to the effects of chemotherapy: an in vitro study. Br J Cancer 2008;99:481–7.
[16] Lee SJ, Oh SJ, Chi DY, Kil HS, Kim EN, Ryu JS, et al. Simple and highly efficient synthesis of 3′-deoxy-3′-[$^{18}$F]fluorothymidine using nucleophilic fluorination catalyzed by protic solvent. Eur J Nucl Med Mol Imaging 2007;34: 1406–9.
[17] Lee SJ, Yang EK, Kim SG. Peroxisome proliferator-activated receptor-gamma and retinoic acid X receptor alpha represses the TGFbeta1 gene via PTEN-mediated p70 ribosomal S6 kinase-1 inhibition: role for Zf9 dephosphorylation. Mol Pharmacol 2006;70:415–25.
[18] Sherley JL, Kelly TJ. Human cytosolic thymidine kinase. Purification and physical characterization of the enzyme from HeLa cells. J Biol Chem 1988;263:375–82.
[19] Mahteme H, Larsson BS, Sundin A, Graf W. 5-FU uptake in liver metastases after intravenous and intraperitoneal administration: an autoradiographic study in the rat. Anticancer Res 1998;18:943–9.
[20] Kim SJ, Lee JS, Im KC, Kim SY, Park SA, Lee SJ, et al. Kinetic modeling of 3′-deoxy-3′-$^{18}$F-fluorothymidine for quantitative cell proliferation imaging in subcutaneous tumor models in mice. J Nucl Med 2008;49:2057–66.
[21] Choi SJ, Kim SY, Kim SJ, Lee JS, Lee SJ, Park SA, et al. Reproducibility of the kinetic analysis of 3′-deoxy-3′-[(18)F]fluorothymidine positron emission tomography in mouse tumor models. Nucl Med Biol 2009;36:711–9.
[22] Xiao Z, Xue J, Sowin TJ, Rosenberg SH, Zhang H. A novel mechanism of checkpoint abrogation conferred by Chk1 downregulation. Oncogene 2005;24:1403–11.
[23] Wong A, Soo RA, Yong WP, Innocenti F. Clinical pharmacology and pharmacogenetics of gemcitabine. Drug Metab Rev 2009;41:77–88.
[24] Hanauske AR, Dittrich C, Otero J. Overview of phase I/II pemetrexed studies. Oncology 2004;18:18–25.
[25] Li LJ, Naeve GS, Lee AS. Temporal regulation of cyclin A-p107 and p33cdk2 complexes binding to a human thymidine kinase promoter element important for G1–S phase transcriptional regulation. Proc Natl Acad Sci USA 1993;90:3554–8.
[26] Tommasi S, Pfeifer GP. Constitutive protection of E2F recognition sequences in the human thymidine kinase promoter during cell cycle progression. J Biol Chem 1997;272:30483–90.
[27] Kinsella AR, Smith D, Pickard M. Resistance to chemotherapeutic antimetabolites: a function of salvage pathway involvement and cellular response to DNA damage. Br J Cancer 1997;75:935–45.
[28] Grem JL, Fischer PH. Enhancement of 5-fluorouracil's anticancer activity by dipyridamole. Pharmacol Ther 1989;40:349–71.
[29] Köhne CH, Hiddemann W, Schüller J, Weiss J, Lohrmann HP, Schmitz-Hübner U, et al. Failure of orally administered dipyridamole to enhance the antineoplastic activity of fluorouracil in combination with leucovorin in patients with advanced colorectal cancer: a prospective randomized trial. J Clin Oncol 1995;13:1201–8.
[30] Pizzorno G, Sun Z, Handschumacher RE. Aberrant cell cycle inhibition pattern in human colon carcinoma cell lines after exposure to 5-fluorouracil. Biochem Pharmacol 1995;49:553–7.
[31] Fraile RJ, Baker LH, Buroker TR, Horwitz J, Vaitkevicius VK. Pharmacokinetics of 5-fluorouracil administered orally, by rapid intravenous and by slow infusion. Cancer Res 1980;40:2223–8.
[32] Yeh KH, Yeh SH, Hsu CH, Wang TM, Ma IF, Cheng AL. Prolonged and enhanced suppression of thymidylate synthase by weekly 24-h infusion of high-dose 5-fluorouracil. Br J Cancer 2000;83:1510–5.
[33] Barthel H, Cleij MC, Collingridge DR, Hutchinson OC, Osman S, He Q, et al. 3′-deoxy-3′-[$^{18}$F]fluorothymidine as a new marker for monitoring tumor response to antiproliferative therapy in vivo with positron emission tomography. Cancer Res 2003;63:3791–8.
[34] Welsh SJ, Titley J, Brunton L, Valenti M, Monaghan P, Jackman AL, et al. Comparison of thymidylate synthase (TS) protein up-regulation after exposure to TS inhibitors in normal and tumor cell lines and tissues. Clin Cancer Res 2000;6:2538–46.
[35] Lee JH, Park JH, Jung Y, Kim JH, Jong HS, Kim TY, et al. Histone deacetylase inhibitor enhances 5-fluorouracil cytotoxicity by down-regulating thymidylate synthase in human cancer cells. Mol Cancer Ther 2006;5:3085–95.